Thermal and Photoreductive Elimination from the Tellurium Center of π-Conjugated Tellurophenes

Elisa I. Carrera, Theresa M. McCormick, Marius J. Kapp, Alan J. Lough, and Dwight S. Seferos*

Department of Chemistry, University of Toronto, 80 St. George Street, Toronto, Ontario, M5S 3H6, Canada

S *Supporting Information*

ABSTRACT: This study introduces small molecule tellurophenes that can undergo photoreductive elimination. A tellurophene compound with strong light absorption properties and extended π-conjugation, 2,5-bis[5-(N,N′-dihexylisoindigo)]tellurophene (**1**), has been synthesized. Halogen oxidative addition to the tellurium center from various halogen sources gives the dibromo- (**1Br$_2$**) and dichloro- (**1Cl$_2$**) adducts, leading to a red-shift in the optical absorption properties. In the presence of excess opposing halogen, **1Br$_2$** and **1Cl$_2$** can interconvert, with equilibrium favoring the dichlorotellurophene adduct. Reductive elimination reactions were studied using optical absorption spectroscopy, NMR spectroscopy, thermogravimetric analysis, and matrix-assisted laser desorption/ionization (MALDI) analysis. Thermal reductive elimination from **1Br$_2$** and **1Cl$_2$** occurs in the solid-state to restore **1**. Photoreductive elimination occurs under irradiation with green (505 nm) light in solution in the presence of a halogen trap with some decomposition. This is the first example of photoreductive elimination from a mononuclear tellurophene complex.
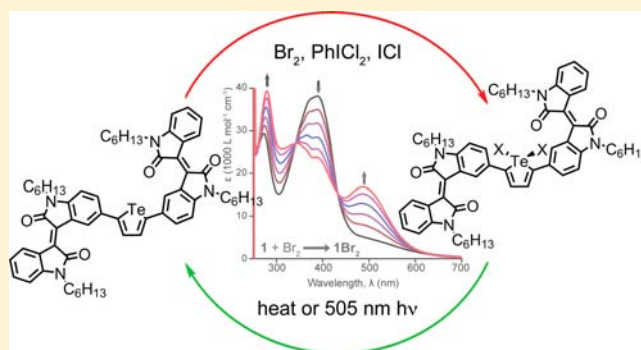
■ INTRODUCTION

Photoreductive elimination is of growing interest for reactions that are important for energy storage such as the generation of H$_2$ from HX or H$_2$O.[1−7] Transition metal complexes are typically used for these types of reactions; however, reactivity is limited by strong M−X bonds which can slow the reductive elimination process. Here we show that a novel isoindigo-substituted tellurophene, 2,5-bis[5-(N,N′-dihexylisoindigo)]-tellurophene (**1**), undergoes facile halogen oxidative addition, thermal reductive elimination (TE), and more importantly photoreductive elimination (PE) using relatively low energy (505 nm) visible light. This is the first example of photoreductive elimination from a mononuclear organotellurium compound, pointing the way toward using main-group p-block elements that are in conjugation with strong organic light absorbers as a means of generating new photoactive and potentially photocatalytic compounds that may be useful in energy storage applications, without the use of expensive late transition metals.

The incorporation of chalcogen (group 16) atoms into organic and inorganic compounds and the properties they impart are being increasingly studied.[8−22] Incorporation of the metalloid tellurium, in particular, leads to interesting reactivity and chemical properties that are not observed in their lighter chalcogen analogues. Organotellurium(II) compounds are converted to organotellurium(IV) adducts with oxidants such as halogens and hydrogen peroxide.[23−25] The resultant Te−X bond formation is reversible which allows for halogen exchange

reactions as well as facile reductive elimination to regenerate the organotellurium(II) species.[23,25,26] Diorganotellurides such as diphenyl telluride behave as oxidants or reductants (depending on the oxidation state of Te) for halogenation and dehalogenation reactions of various organic substrates.[27] Reductive elimination can also be induced thermally as observed for tellurapyrylium dyes.[25,26] The ability to shuttle between Te(II) to Te(IV) offers potential for catalysis, and some organotellurium compounds have been used as catalysts for organic transformations.[28−34]

Tellurophene, the tellurium analogue of thiophene, is of interest as an organic electronic material due to favorable optoelectronic properties such as a narrow optical gap, large dielectric constant, high polarizability, and the ability to form close intramolecular interactions.[35−45] The reactivity of the tellurium center and its potential utility as a catalyst, however, have not been extensively studied. Our group has reported the oxidative addition of bromine to a tellurium-containing polymer[12] and 2,5-substituted tellurophene small molecule with extended π-conjugation.[11] Thermal reductive elimination was observed for the polymer. On the basis of their strong light-absorbing properties, we hypothesize that the reactivity of the tellurium atom as part of 2,5-disubstituted tellurophene small molecules should be of particular interest for light-driven transformations.
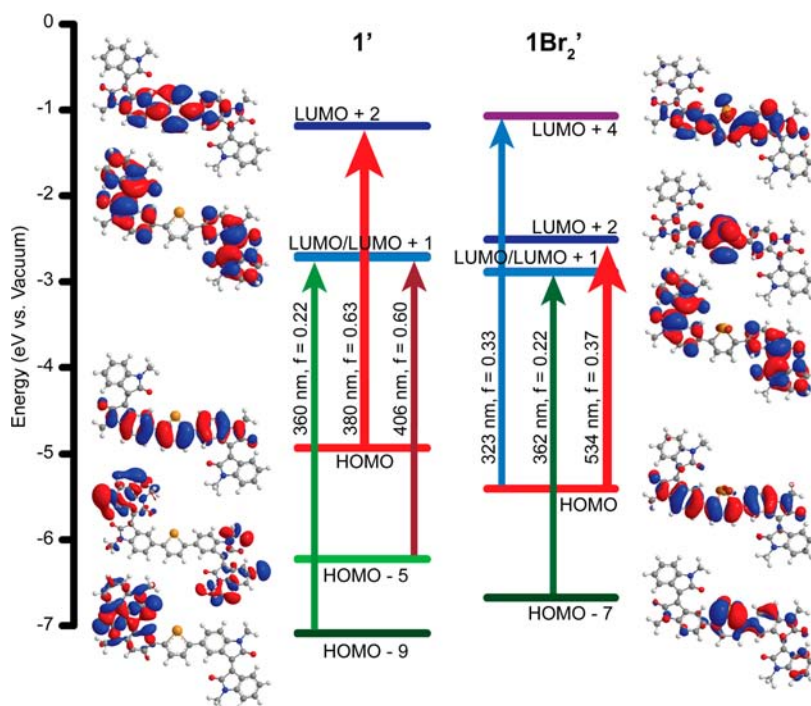
Figure 1. The main transitions of **1**′ and **1Br₂**′ with oscillator strengths greater than 0.2 predicted by TD-DFT and their associated MOs (isocontour value of 0.02). Excludes transitions at 248 nm ($f = 0.42$) and 249 nm ($f = 0.22$) in **1**′ and **1Br₂**′, respectively. The nearly degenerate LUMO and LUMO + 1 MOs have been superimposed for simplification.

Improving the photoreductive elimination of X_2 from late transition metal complexes has attracted significant recent attention.[46−51] The vast majority of these are dinucluear systems containing two precious metals, with quantum yields ranging from 0.29% to 38%. Gabbaï and co-workers have shown that one of the transition metals in a bimetallic system can be replaced by the main group element tellurium to give a main group/late transition metal Te(III)−Pt(I) complex.[52] This dinuclear complex can oxidatively add and photoreductively eliminate halogens with a quantum yield of 4.4%. This sole example of PE from an inorganic tellurium center provides motivation for studying this process in mononuclear organotellurium compounds, such as tellurophene, removing transition metals from the system altogether. The ability to design tellurophenes with extended π-conjugation and strong light-absorbing properties makes these compounds even more attractive due to the possibility of undergoing PE using low energy light. Successful PE from such compounds would provide the opportunity to explore the utility of tellurophenes as catalysts for energy storage reactions.

Herein, we report a new, strong light-absorbing isoindigo-containing tellurophene. The extended π-conjugation of this tellurophene and resultant low-energy absorption introduces the possibility for PE using relatively low-energy light. The photophysics and calculated electronic structure of this compound are determined, the reactivity with various halogen sources is evaluated, and the TE and PE reactions are studied.

■ RESULTS AND DISCUSSION

Computational Modeling. Density functional theory (DFT) was used to calculate the model compound 2,5-bis[5-(N,N′-dimethylisoindigo)]tellurophene (**1**′) and its halogenated adducts **1Br₂**′ and **1Cl₂**′ prior to synthesis. The hexyl chains were replaced with methyl groups to reduce computa-

tional time. Geometry optimizations and time-dependent (TD-DFT) calculations[53] were performed using the Gaussian 09 software package[54] at the B3LYP level of theory[55−57] with a split basis set (LANL2DZ for tellurium,[58] and 6-31G (d) for all other atoms[59]). Compound **1**′ has a calculated −4.92 eV HOMO energy level (relative to vacuum) and a calculated 2.21 eV HOMO−LUMO energy gap. The molecular orbital (MO) diagram of the HOMO shows electron density across the length of the molecule, which is consistent with a delocalized electronic structure (Figure 1). The LUMO and LUMO + 1 MOs are more localized, with the majority of electron density residing in the π* orbitals of each isoindigo unit, respectively (the MO diagrams have been superimposed in Figure 1 for simplification). These MOs are essentially degenerate (−2.71 and −2.70 eV, respectively). Upon bromination, the HOMO energy level is stabilized significantly (by 0.50 eV; to −5.41 eV), while the LUMO energy level is stabilized only slightly (by 0.18 eV; to −2.52 eV), leading to an overall increase in the HOMO−LUMO energy gap upon bromination (2.89 eV). Similar to compound **1**′, the HOMO of **1Br₂**′ is a delocalized π-state, while electron density is localized on the π* orbitals of each isoindigo unit for the nearly degenerate LUMO and LUMO + 1 MOs (−2.89 and −2.88 eV, respectively).

TD-DFT calculations were performed on **1**′ and **1Br₂**′ to determine the excited state transitions (Figure 1; see Figure S1 for the calculated absorption spectra). The HOMO → LUMO transition is not expected to contribute significantly to the absorption spectrum of **1**′ due to an extremely low oscillator strength ($f < 0.01$, 703 nm). Instead, the main transition (the transition with highest oscillator strength) is the 13th excited state which occurs at 380 nm ($f = 0.63$), which is HOMO → LUMO + 2 in nature. The MO diagrams indicate that this is a delocalized $\pi \rightarrow \pi^*$ transition. The HOMO → LUMO transition in **1Br₂**′ occurs at a higher energy than **1**′ (597 nm)

Scheme 1. Synthetic Route to 2,5-Bis[5-(N,N′-dihexylisoindigo)]tellurophene (1)
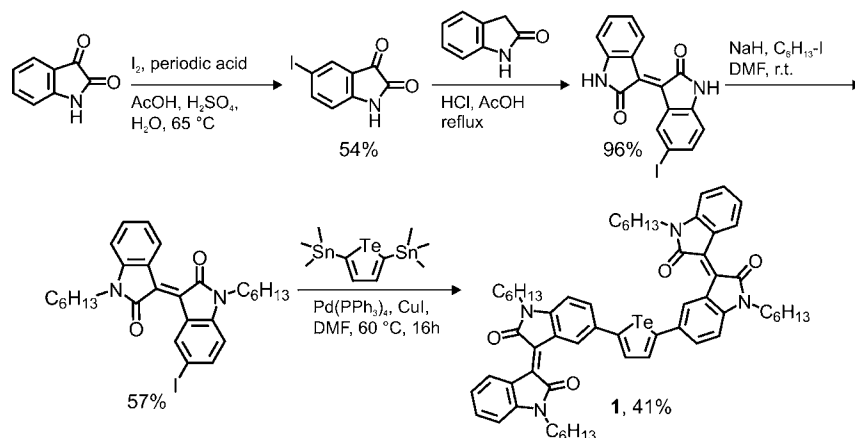
Scheme 2. Oxidative Addition of Br₂, PhICl₂, or ICl To Afford 1Br₂ and 1Cl₂ and Reductive Elimination by Heat or Light
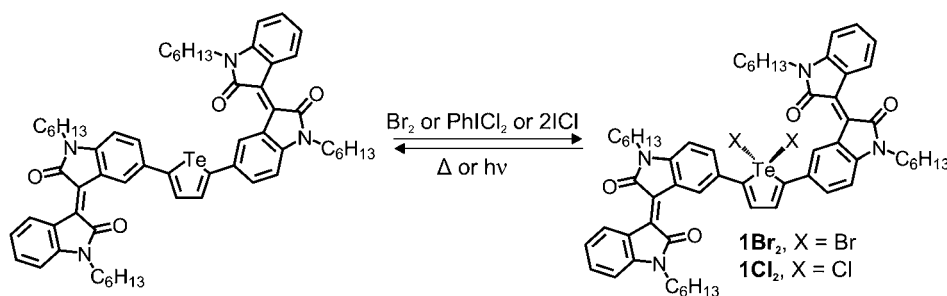
which is consistent with an increase in the HOMO−LUMO energy gap. However, the oscillator strength of this transition is too low to contribute significantly to the absorption spectrum ($f = 0.03$). The main transition (3rd excited state) is a HOMO → LUMO + 2 transition at 535 nm (f = 0.37), which is red-shifted compared to **1′** due to a large stabilization of the LUMO + 2 energy (by 1.33 eV). The MO diagrams indicate that this transition has charge transfer character, from a delocalized π-state in the HOMO to localized electron density on the dibromotellurophene in the LUMO + 2, consistent with a donor−acceptor type structure.[20,60,61] Higher energy transitions with significant oscillator strength also contribute to the calculated electronic spectra of **1′** and **1Br₂′** (see Figure 1). Similar results are obtained for **1Cl₂′** (Figure S2, Supporting Information).

Interestingly, some electron-density in the LUMO + 2 state for **1Br₂′** (the strongest predicted transition) resides within the Te−Br antibonding orbitals. This suggests that populating this state (i.e., through photoexcitation) may induce reductive elimination, which has previously been reported for Te−Pt complexes[52] but never for a tellurophene. Because of the strong light-absorbing isoindigo units and extended π-conjugation, the use of visible light to induce reductive elimination from the tellurophene can be studied.

Synthesis. The synthetic route utilizes N,N′-dihexyl-5-iodoisoindigo for coupling with a 2,5-difunctionalized tellurophene (Scheme 1). Accordingly, 5-iodoisatin was prepared by treating isatin with I₂ and periodic acid under acidic conditions[62] (54% yield). Condensation[63] between 5-iodoisatin and oxindole in acetic and hydrochloric acid afforded 5-iodoisoindigo in 96% yield. Finally, 5-iodoisoindigo was hexylated at the N positions by treatment with sodium hydride followed by the addition of iodohexane[64] to afford N,N′-

dihexyl-5-iodoisoindigo in 57% yield. Hexyl chains are required for solubility due to the strong pi-stacking of isoindigo-type conjugated molecules.[63] The target compound 2,5-bis[5-(N,N′-dihexylisoindigo)]tellurophene (**1**) was prepared through a Stille-type coupling between N,N′-dihexyl-5-iodoisoindigo and 2,5-bis(trimethylstannyl)tellurophene (prepared from literature methods[65,66]) to afford the desired product in 41% yield.

Oxidative Addition and Competition Experiments. The absorption spectrum of compound **1** in chloroform shows a dual-band absorption with peaks occurring at 274 and 390 nm, respectively. The charge-transfer nature of the lower energy transition (as calculated by DFT) was probed by obtaining the absorption spectrum of **1** in solvents of increasing polarity;[61,67] however, solvatochromism was not observed in the absorption spectra (Figure S3, Supporting Information). Since solvatochromic effects are a result of the excited state nature of the compound, solvatochromism is more commonly observed in fluorescence spectroscopy; however, **1** does not exhibit appreciable emission to study this phenomenon due to the heavy atom effect imparted by tellurium.[68,69]

Halogen addition to **1** was attempted using various halogen sources: bromine (Br₂), iodobenzene dichloride[70] (PhICl₂), iodine (I₂), and iodine monochloride (ICl) (Scheme 2). Dramatic color changes are observed upon Br₂ and PhICl₂ addition, from yellow (for a dilute solution of **1**) to red and reddish-orange for the bromine and chlorine adducts, respectively. Stoichiometric optical absorption titration experiments indicate clean conversion from **1** (λ_{max} = 389 nm, $\varepsilon = 3.8 \times 10^4$ L cm⁻¹ mol⁻¹) to the halogenated adducts by the presence of clear isosbestic points (340 and 431 nm for Br₂ titration, 323 and 430 nm for PhICl₂ titration; Figure 2a,b). Complete conversion to **1Br₂** and **1Cl₂** is achieved after the addition of 1.25 equiv of Br₂ and PhICl₂, respectively. **1Br₂** and
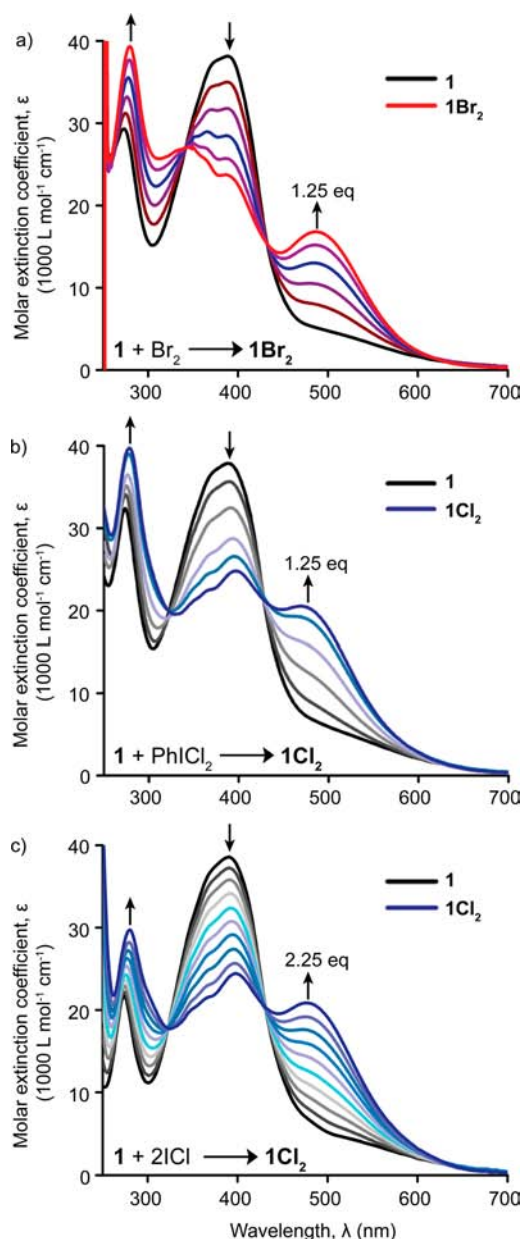
Figure 2. Optical absorption spectra of **1** treated with (a) Br$_2$ in carbon tetrachloride, (b) PhICl$_2$ in chloroform, and (c) ICl in chloroform in 0.25 equiv increments.

1Cl$_2$ both exhibit a red-shift in absorption compared to **1**, with the lowest energy maxima at 486 nm ($\varepsilon = 1.7 \times 10^4$ L cm^{-1} mol^{-1}) and 471 nm ($\varepsilon = 2.0 \times 10^4$ L cm^{-1} mol^{-1}), respectively. Several higher energy absorption maxima are also observed, which is consistent with the TD-DFT calculations. The slight excess of halogen required for complete conversion is likely due to halogen loss from either evaporation or reaction with solvent. Immediate addition of 1 equiv of Br$_2$ from a more concentrated stock solution to **1** shows complete conversion at 1 equiv by ^{1}H NMR spectroscopy (Figure S4a, Supporting Information).

Upon addition of the mixed halogen, ICl, an immediate color change to reddish-orange is observed. A titration experiment shows that complete conversion is achieved at 2.25 equiv, and the absorption spectrum of the product is identical to **1Cl$_2$** (Figure 2c). This is further confirmed by ^{1}H NMR spectros-

copy, where the addition of 1 and 2 equiv of ICl give 50% and 100% conversion, respectively, to a product that is spectroscopically identical to **1Cl$_2$** (Figure S4b, Supporting Information). No reaction was observed for I$_2$.

To confirm the addition of two chlorine atoms to Te from ICl, a crystal structure of the phenyl-substituted analogue, 2,5-bis(phenyl)dichlorotellurophene (**2Cl$_2$**) was determined by X-ray crystallography (attempts to obtain crystal structures of **1Br$_2$** and **1Cl$_2$** were unsuccessful). Orange block crystals of **2Cl$_2$** were obtained by allowing a solution of **2** in chloroform to slowly diffuse into a solution of 2 equiv of ICl in carbon tetrachloride (Figure 3). The structure confirms the addition of
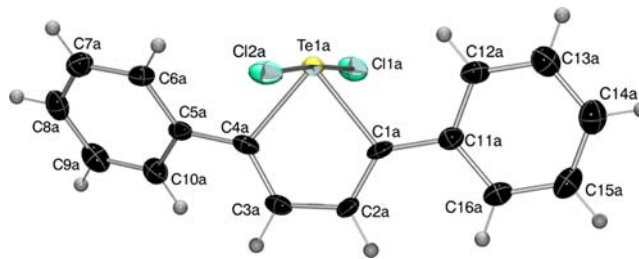

Figure 3. ORTEP drawing of compound **2Cl$_2$A** shown at 50% probability.

two chlorine atoms to the tellurium center. Two molecules of **2Cl$_2$** are in the asymmetric unit (**2Cl$_2$A** and **2Cl$_2$B**; Figure S5, Supporting Information), with the major difference being the dihedral angles between the phenyl rings and the tellurophene ring.

Competition experiments were carried out where Br$_2$ was added to solutions of **1Cl$_2$** and ICl was added to solutions of **1Br$_2$**. The progress of the reaction was monitored through optical absorption spectroscopy (Figure 4). In both cases, addition of excess opposing halogen readily yields the corresponding opposing halogen adduct, demonstrating that halogen addition is reversible, and an equilibrium exists between the two halogen adducts. Clear isosbestic points are observed in the competition experiments, indicating direct conversion from one halogenated adduct to the other. Approximately 10 equiv of Br$_2$ is required to convert **1Cl$_2$** to **1Br$_2$**, while 2.5 equiv of ICl is required to convert **1Br$_2$** to **1Cl$_2$**. Given that 2.25 equiv of ICl was required to initially convert **1** to **1Cl$_2$**, 2.5 equiv is only a slight excess to carry out the exchange reaction. On the other hand, exchange for Br$_2$ requires a much larger excess. Stronger bonds for Te−Cl as compared to Te−Br have been experimentally observed for other organotellurium compounds[23] and explains the trends in the exchange reactivity. Elemental analyses of **1**, **1Br$_2$**, and **1Cl$_2$** (prepared with ICl) confirm the identity of each compound but also indicate the presence of water which is likely the result of hydrogen bonding between water and the two isoindigo units.

Electrochemical Behavior. The positions of the frontier orbital energies of **1** and **1Br$_2$** were determined by cyclic voltammetry (Figure S6, Table S3, Supporting Information). The HOMO and LUMO energy levels of **1** occur at −5.37 eV and −3.60 eV, and the HOMO and LUMO energies of **1Br$_2$** occur at −5.76 eV and −3.59 eV versus vacuum, respectively. When **1** is converted to **1Br$_2$**, the oxidation potential shifts to a higher potential and is irreversible, while the reduction potential is roughly equal to **1** and is quasi-reversible. As a result, the HOMO−LUMO gap increases from 1.77 to 2.17 eV
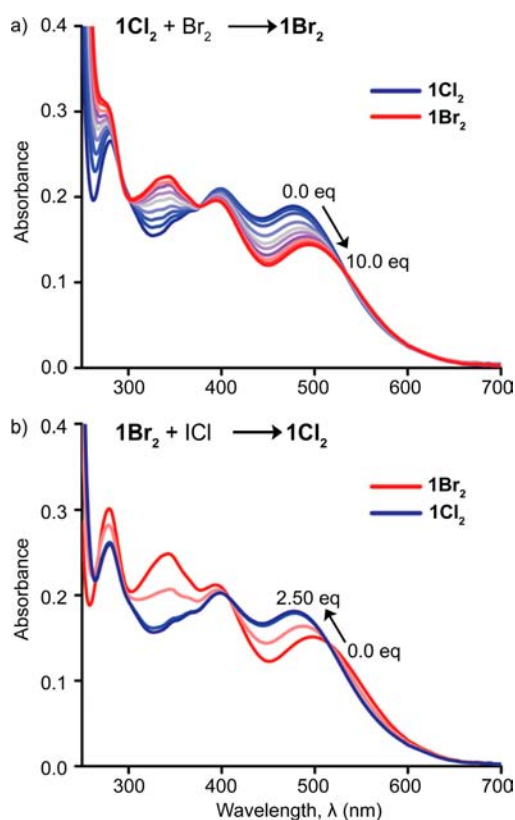
Figure 4. Optical absorption spectra of competition experiments in chloroform (a) **1Cl₂** treated with Br₂, and (b) **1Br₂** treated with ICl.

upon bromination which is consistent with the trends in the DFT-calculated MO energy levels.

Thermal Reductive Elimination. Initial thermolysis reactions were attempted for solutions of **1Br₂** in CCl₄ with 1-hexene as a halogen trap and monitored by optical absorption

spectroscopy; however, no reductive elimination was observed for temperatures just below the boiling point of the solvent (70 °C). Solid-state thermolysis experiments were carried out instead on **1Br₂**, **1Cl₂**, and **1** (used as a control). Thin films of the compounds were heated on a hot plate set to 140 °C in air, and the solid state optical absorption spectra were recorded at several time intervals (Figure S7, Supporting Information). Within 10 min, a significant change is observed in the optical absorption spectra of **1Br₂** and **1Cl₂**. The intensity of the low energy peak in the halogenated adduct decreases, while a peak at 389 nm, corresponding to the λ_{max} of **1**, increases. The solid state optical absorption spectra of **1Br₂** and **1Cl₂** are identical to **1** at the end of the experiment (Figure 5). In control experiments, only a slight decrease in intensity of the λ_{max} of **1** is observed during heating (Figure S8a, Supporting Information).

^{1}H NMR spectroscopy experiments were carried out to further confirm the chemical transformations observed when **1Br₂** and **1Cl₂** are heated in the solid state. Solids of **1Br₂** were heated to 140 °C in air as well as under a nitrogen atmosphere. After 1 h of heating in air, the sample contained a mixture of **1** and the brominated compound (∼60:40 **1**/**1Br₂** by integration of tellurophene protons; Figure S9, Supporting Information), along with new aromatic resonances that we assign as minor decomposition products. Further heating led to nearly complete disappearance of **1Br₂** and restoration of **1** with some decomposition (Figure 5b). After 1 h of heating under nitrogen, more complete conversion to **1** (∼80:20 **1**/**1Br₂**) was observed, with a few new aromatic signals corresponding to decomposition products (Figure S9, Supporting Information). It should be noted, however, that some of the decomposition products from the sample heated under nitrogen were not soluble in CDCl₃ and are therefore not observed in the NMR spectrum. Insoluble material was not observed for the sample heated in air. The integration of some of the isoindigo protons relative to the tellurophene protons are too high in the restored
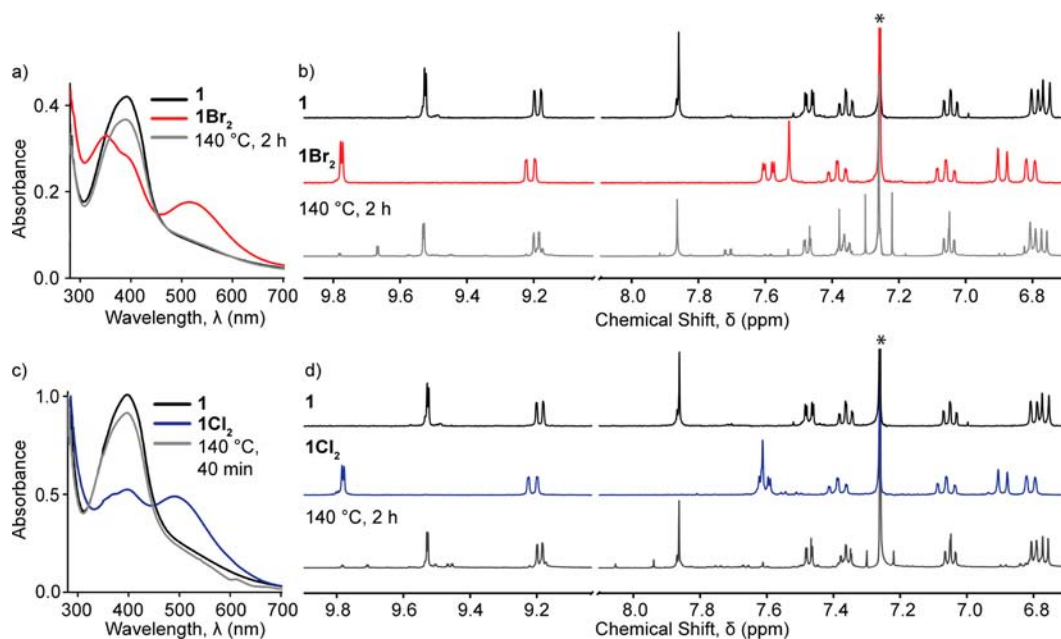

Figure 5. Solid-state optical absorption spectra of **1Br₂** (a) and **1Cl₂** (c) before and after heating at 140 °C. Compound **1** is included for reference. ^{1}H NMR spectra (aromatic region) of **1Br₂** (b) and **1Cl₂** (d) before and after heating at 140 °C under air and nitrogen. Compound **1** is included for reference. The CDCl₃ residual peak is marked by asterisks.
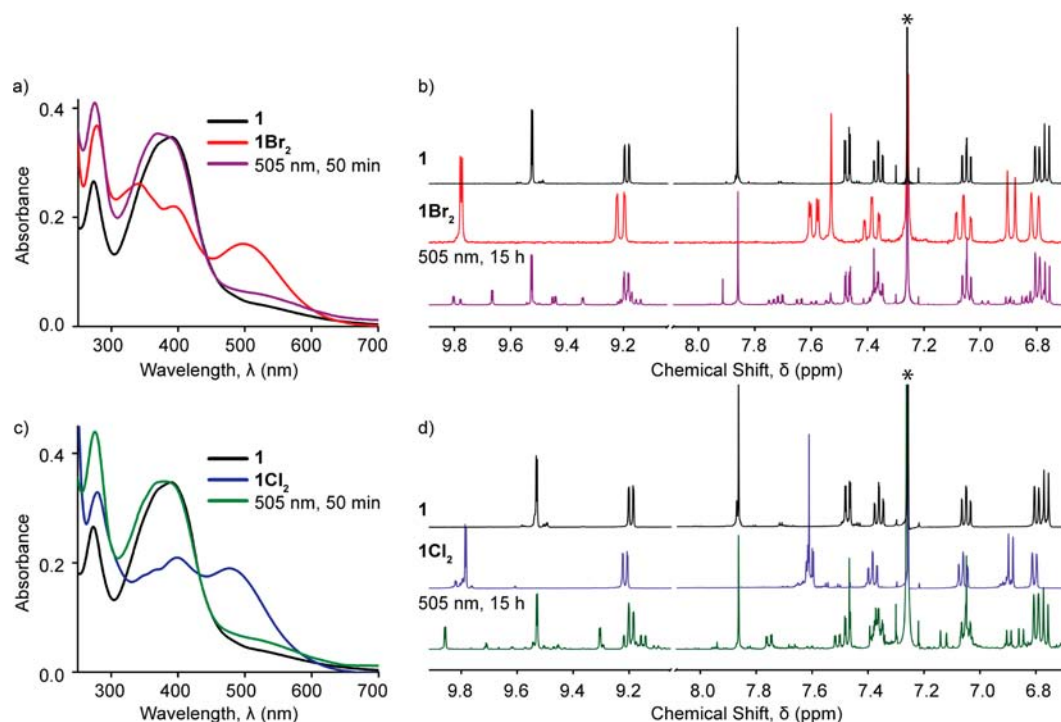
Figure 6. Optical absorption spectra of **1Br$_2$** (a) and **1Cl$_2$** (c) before and after irradiation with 505 nm light under nitrogen atmosphere. Compound **1** is included for reference (normalized to spectrum of PE product at 390 nm). ^{1}H NMR spectra (aromatic region) of **1Br$_2$** (b) and **1Cl$_2$** (d) before and after after irradiation with 505 nm light under nitrogen atmosphere. Compound **1** is included for reference. The CDCl$_3$ residual peak is marked by asterisks.

compound. For example, integrating the tellurophene protons to 1.0, isoindigo protons that should integrate for 1.0 instead integrate for 1.4 or 1.7 (see Figure S11a, Supporting Information for proton integrations). This suggests that some of the decomposition products may have common resonances that cannot be distinguished from **1**. **1** is stable at 140 °C in air (Figure S8b, Supporting Information), which suggests that the liberated halogens play a role in the decomposition pathway.

These experiments were repeated at lower temperature (hot plate set to 120 °C) to determine whether TE could occur with less decomposition (Figure S10, Supporting Information). The reaction proceeds notably more slowly (over ~5 h). Once again, more complete conversion occurs under nitrogen for a given amount of time (~90:10 **1/1Br$_2$** compared to ~55:45 in air); however relative integrations of isoindigo protons to tellurophene protons are similar to the experiment carried out at 140 °C. Even at lower temperature, it appears that some decomposition and insoluble material occur.

Similar results were obtained with **1Cl$_2$**, except that neither experiment (air vs nitrogen atmosphere) led to insoluble products. As a result, all of the decomposition products are observed by ^{1}H NMR spectroscopy, which shows a significantly greater amount of decomposition in the sample heated under nitrogen compared to the sample heated in air. Less complete conversion was again observed after heating for 1 h in air compared to nitrogen (Figure S9b, Supporting Information). Further heating in air (2 h total) led to nearly complete conversion to **1** (Figure 5d) with some decomposition as indicated by the high isoindigo proton integration compared to the tellurophene protons. Interestingly, the minor decomposition products appear to be different for the **1Br$_2$** and **1Cl$_2$** experiments (Figure S11a, Supporting Information), which

further suggests that the liberated halogen plays a role in the decomposition pathway.

To further confirm TE, thermogravimetric analysis (TGA) was performed on **1** (as a control), **1Br$_2$**, and **1Cl$_2$** prepared from ICl. The samples were heated to 200 °C (5 °C/min) and held at this temperature for 2 h (Figure S12, Supporting Information). The mass of **1** remained stable over the entire experiment. For **1Br$_2$** and **1Cl$_2$**, the weight percent values at the end of the experiment were 85.1% and 95.4%, respectively, which are in good agreement with the expected mass loss for halogen elimination to restore **1** (expected values are 86.6% and 93.6%, respectively). In addition, TGA further confirms the formation of **1Cl$_2$** from ICl as opposed to a mixed halogen adduct since the corresponding mass loss would vary dramatically for a I–Te–Cl adduct.

Overall, TE occurs slowly at 120 °C and more rapidly at 140 °C, with some decomposition occurring at both temperatures. On the basis of the differences in the ^{1}H NMR spectra, these decomposition products are the same regardless of the atmosphere of the experiment but are different for the bromine and chlorine adducts. Surprisingly, a greater amount of decomposition occurs when the samples are heated under nitrogen than in air, leading to insoluble material (in the case of thermolysis of **1Br$_2$**) or the observation of significant decomposition products in the ^{1}H NMR spectrum (in the case of thermolysis of **1Cl$_2$**). This suggests that oxygen may be involved in a process that is in competition with the decomposition pathway. Oxygen can react with halogen species to form unstable halogen oxides of various X$_n$O compositions.[71,72] In this way, oxygen may act as a trap for liberated halogens during the TE process, preventing reaction with **1** to form decomposition products. This competing pathway is removed when the experiment is carried out under nitrogen,

and a greater amount of decomposition is observed. Further discussion of the decomposition products are provided below.

Photoreductive Elimination. Photolysis experiments were carried out using a 505 nm light-emitting diode (LED) light source. This wavelength coincides with the long wavelength absorption maximum for the halogenated adducts and was used to selectively excite that species. Solutions of **1Br$_2$** and **1Cl$_2$** were prepared in chloroform (1×10^{-5} M) with 1-hexene as a halogen trap (0.1 M). The solutions were irradiated and monitored periodically by optical absorption spectroscopy both under nitrogen and ambient conditions (Figures S13 and S14, Supporting Information). The optical absorption spectra of the photolysis products of **1Br$_2$** and **1Cl$_2$** are similar. As was observed in the thermolysis experiments, the intensity of the low energy absorption corresponding to the halogenated adduct decreases, while the absorption near 390 nm intensifies as the sample is irradiated. By the end of the experiment, however, a low intensity absorption near 520 nm remains, and a shifted λ_{max} (relative to **1**) occurs at 365 nm (Figure 6). The high energy absorption around 275 nm intensifies with photolysis, which indicates a possible contribution from decomposition products; however, the shoulder at 390 nm suggests that restored **1** is also present. A slight decrease in the intensity of the absorption at 365 nm (from decomposition products) is observed for the sample irradiated under nitrogen compared to air for both **1Br$_2$** and **1Cl$_2$**; however the spectra are very similar (Figure S14c,d, Supporting Information). Overall, the optical absorption spectra suggest that PE occurs but also leads to the formation of decomposition products both in air and under nitrogen. The optical absorption spectrum of **1** after irradiation shows a slight decrease in intensity compared to before irradiation but is otherwise identical (Figure S15a, Supporting Information).

Photolysis experiments were also carried out on more concentrated solutions (~2 mg/mL) under dry, oxygen-free conditions for analysis by ^{1}H NMR spectroscopy. In order to reduce the reaction time, the concentration of 1-hexene was increased to 2 M, and the solution was irradiated overnight, after which the solvent and excess trap were removed by evaporation, and the products were redissolved in CDCl$_3$. A comparison of the ^{1}H NMR spectra of **1** and the halogenated adducts before and after photolysis clearly shows the disappearance of the halogenated compound and the restoration of signals from **1** (Figure 6). For the photolysis of both **1Br$_2$** and **1Cl$_2$**, new aromatic signals appear. Some of these resonances overlap with the isoindigo proton signals from restored **1**, which causes the isoindigo proton integrations to be significantly higher than the tellurophene proton integrations. The ^{1}H NMR spectra once again show that the decomposition products are not the same for **1Br$_2$** and **1Cl$_2$** (see Figure S11b, Supporting Information for a comparison of spectra including relative integrations). In a control experiment, irradiation of **1** for 18 h led to a small amount of decomposition (Figure S15b, Supporting Information) as indicated by isoindigo proton integrations that are slightly high relative to the tellurophene protons.

In order to further confirm that reductive elimination is light-driven in these experiments, a solution of **1Br$_2$** and 1-hexene was kept in the dark for an equal amount of time as the photolysis experiment. The ^{1}H NMR spectrum does not show any evidence for the restoration of **1** in the absence of light. Next, a solution of **1Br$_2$** and 1-hexene was irradiated at 0 °C. The ^{1}H NMR spectrum indicates that **1Br$_2$** is no longer

present; however, the sample contains decomposition products rather than restored **1** (Figure S16, Supporting Information). The disappearance of **1Br$_2$** shows that reductive elimination of the halogens from Te is a light-driven rather than a thermal pathway. The reaction between free halogen and 1-hexene is slower at cooler temperature, leading to decomposition products rather than restored **1**.

The use of a more reactive halogen trap, 2,3-dimethyl-1,3-butadiene (DMBD), during photolysis of **1Br$_2$** leads to conversion at much shorter irradiation times and with less decomposition. The ^{1}H NMR spectrum after 5 h of irradiation under nitrogen atmosphere shows some new aromatic proton resonances, similar to those observed in the 1-hexene photolysis experiment. The relative integrations of the isoindigo protons to the tellurophene protons are still higher than in **1** but much less so than in experiments with 1-hexene as the trap, indicating that decomposition products are present but in a much lesser amount (Figure S17a, Supporting Information). The greater reactivity of DMBD with halogens compared to 1-hexene makes it a more effective halogen trap, limiting unwanted reactions between liberated halogens and the tellurophene compounds. The optical absorption spectrum of the photolysis of a dilute solution of **1Br$_2$** with 0.1 M DMBD under nitrogen is similar to that of the 1-hexene experiment, indicating both the presence of restored **1** and some decomposition products (Figure S17b, Supporting Information).

Mechanistic studies on TE of halogens from organotellurium compounds suggest a unimolecular mechanism is more probable than a bimolecular mechanism.[26] In this case, steady-state intermediates were not observed spectroscopically upon PE from Te(IV) to Te(II), which would suggest a unimolecular PE pathway, although a bimolecular radical mechanism cannot be discounted. If such a mechanism occurs, it would involve the formation of the unstable Te(III) intermediate, which would likely be too short-lived to observe using standard NMR and optical absorption spectroscopy.

To quantify the efficiency of the PE reactions, the photochemical quantum yields were determined using potassium ferrioxalate standard actinometry.[73−75] Using DMBD as the halogen trap at a concentration of 2 M, the quantum yields for PE of **1Br$_2$** and **1Cl$_2$** are 0.18% (std = 0.01) and 0.19% (std = 0.04), respectively. To put these numbers into context, they are lower than those obtained with recent bimetallic gold and platinum complexes[49−51] but similar to those obtained with recent bimetallic rhodium complexes.[47]

The long irradiation times and low quantum yields, even with the more reactive DMBD trap, indicate that the reaction is not very efficient. As previously discussed, the main transitions in the parent and halogenated compounds are HOMO → LUMO + 2 transitions. The existence of lower energy excited states that do not contain Te−X antibonding character may limit PE.

Discussion of Decomposition Products. In attempts to determine the decomposition products, several observations were made: (1) Decomposition products are not the same for **1Br$_2$** and **1Cl$_2$** in the TE experiments; (2) decomposition products are not the same for **1Br$_2$** and **1Cl$_2$** in the PE experiments; (3) there are some common ^{1}H NMR signals between the TE and PE decomposition products for a given adduct; (4) more decomposition (and more decomposition species) occurs for PE compared to TE; (5) the isoindigo protons integrate too high compared to the tellurophene

protons following reductive elimination, and this discrepancy is more pronounced in the PE experiments.

Several types of decomposition products are possible from these reactions. The high temperature or radiative environment may provide favorable conditions in which free halogens can react with **1** at sites other than the tellurium center, such as the aromatic carbons of the isoindigo units. In this case, halogenation of the isoindigo unit(s) would likely result in dramatic changes in the resonances of the remaining isoindigo protons. The low intensity decomposition peaks in the ^{1}H NMR spectra (6.8−6.9, 7.5−8.0 ppm) are likely a result of these types of decomposition products. The resonances of these protons may also be different depending on the type of halogen that is appended to the isoindigo unit, which is consistent with the observed difference in decomposition products for **1Br₂** and **1Cl₂** in the isoindigo region of the spectrum.

The appearance of overlapping resonances with the isoindigo proton resonances indicates that some of decomposition products have similar isoindigo environments to **1**. This, in conjunction with the low tellurophene proton integration relative to isoindigo, suggests two other possible types of decomposition products: tellurophene halogenated at the C3 or C4 position(s) or a ring-opened product. In both of these cases, the positions of the isoindigo proton resonances would likely not change dramatically, and the integration of the tellurophene protons would be lower than expected for **1**. Halogenation at both C3 and C4 positions of the tellurophene would lead to a loss of the tellurophene proton signal, while halogenation at only one of these positions would shift the tellurophene proton signal and reduce the integration by one proton. The observation of a new singlet near the tellurophene signal in the ^{1}H NMR spectra (more pronounced for some experiments than others) may be due to a C3 or C4 mono-halogenated tellurophene. A ring opened product would lead to a loss of the tellurophene proton signals. A combination of decomposition products is also possible (e.g., ring-opened and halogenated).

Matrix-assisted laser desorption/ionization (MALDI) analysis was performed on the TE and PE products of **1Br₂** and **1Cl₂**. In all cases, a high intensity m/z peak corresponding to the parent compound **1** is observed (m/z = 1038), further confirming that both TE and RE occur. Several other signals are also observed (Table S4, Supporting Information), including those corresponding to (1) a ring-opened, mono-halogenated product (- Te + 1X); (2) a ring-opened, di-halogenated product (- Te + 2X); (3) a mono-halogenated tellurophene product (**1** + X); (4) a di-halogenated tellurophene product (**1** + 2 X, for **1Cl₂** photolysis only). For **1Br₂**, the intensity of the ring-opened dihalogenated signals are comparable for both the TE and PE experiments; however, a greater amount of mono-halogenated tellurophene is observed in the PE experiment. For **1Cl₂**, the intensity of the ring-opened product signals are significantly higher in the PE experiment compared to TE and are also significantly higher for the photolysis of **1Cl₂** compared to **1Br₂**. On the basis of these observations, several possible decomposition products are proposed (Figure S18, Supporting Information). We have also performed mass analysis on the insoluble material obtained from thermolysis of **1Br₂** under nitrogen. The absence of signals at double or triple the molecular weight of **1** indicates that oligomers are not formed as a decomposition product.

Irradiation of **1Br₂** in the absence of halogen trap leads to complete disappearance of **1Br₂** but very little restored **1** as

indicated by the tellurophene proton signal. The ^{1}H NMR spectrum shows that the major decomposition product for photolysis carried out with and without a halogen trap contain common resonances (Figure S19, Supporting Information). Additional minor aromatic signals are also observed including a singlet at 7.92 ppm which may be due to a tellurophene decomposition product. Peaks corresponding to the mass of a ring-opened dibrominated compound (m/z = 1069.4) and a monohalogenated tellurophene product (m/z = 1117.3) are once again observed by mass spectrometry.

■ CONCLUSION

We have synthesized a new tellurophene compound, 2,5-bis[5-(N,N'-dihexylisoindigo)]tellurophene, that has strong light-absorbing properties and extended π-conjugation. The oxidative addition of halogens to the tellurium center and both thermal and photoreductive elimination were studied. The dibromo- and dichloro-Te(IV) compounds are rapidly formed and can be readily isolated. These compounds undergo halogen-exchange reactions in solutions containing excess opposing halogen, demonstrating that in the case of tellurophene, the Te−X bond is labile. Compounds **1Br₂** and **1Cl₂** undergo TE and PE to restore compound **1**; however, both reductive elimination pathways also lead to the formation of decomposition products. The reactivity of the halogen trap influences the reaction rate as well as the extent of decomposition, with shorter times and less decomposition observed for the more reactive DMBD trap. Several types of decomposition products have been observed by ^{1}H NMR spectroscopy and mass spectrometry of the TE and PE products. This is the first detailed study of TE from a tellurophene center and the first example of PE from a mononuclear organotellurium compound. Despite the shortcomings of this particular system, we achieve PE efficiencies that are close to certain binuclear late transition metal complexes. Changing the flanking substituents so that the main transition is HOMO → LUMO should improve the PE efficiency by removing efficiency losses from relaxations that do not promote Te−X dissociation. Preliminary work from our laboratory is yielding promising results along these lines, which will be the subject of a future publication. The realization of more efficient PE of halogens from organotellurium compounds could lead to transition metal-free catalysts for energy storage reactions.

■ EXPERIMENTAL SECTION

General Considerations. All reagents were used as received. Isatin, oxindole, periodic acid, sodium hydride, iodohexane, palladium tetrakis(triphenylphosphine) (Pd-(PPh₃)₄), iodine monochloride (ICl), 1-hexene, 2,3-dimethyl-1,3-butadiene, bromine, chloroform, and carbon tetrachloride were purchased from Sigma-Aldrich. Sulfuric acid, acetic acid, DMF, MgSO₄, and NaHCO₃ were purchased from Fisher Scientific. Iodine and hexanes were purchased from Caledon. CuI and ethyl acetate were purchased from Alfa Aesar and EMD, respectively. Silica gel was purchased from Silicycle. Tellurophene,[65] 2,5-bis(trimethylstannyl)tellurophene,[66] iodo-benzene dichloride,[70] and 2,5-bis(phenyl)tellurophene[11] were synthesized according to literature procedures.

Optical absorption spectroscopy was carried out using a Varian Cary 5000 UV−vis-NIR spectrophotometer. NMR spectra were recorded on a Varian Mercury 300 spectrometer

(300 MHz), Varian Mercury 400 spectrometer (400 MHz) or Agilent DD2 500 MHz spectrometer as noted. Mass spectrometry was performed using a Waters GCT Premier TOF mass spectrometer. MALDI-TOF was carried out on a Waters MALDI micro MX using a 10000:1 dithranol matrix/analyte ratio. Electrochemistry was carried out using a BASi Epsilon potentiostat. Thermogravimetric analyses were performed on a TA Instruments SDT Q600 Simultaneous TGA/DSC.

Computational Methods. DFT calculations were performed using the Gaussian 09 Software package,[54] at the B3LYP level of theory[56,57] with a split basis set (LANL2DZ for Te[58] and 6-31G (d) for all other atoms[59]). Structures were created using Gaussview 5.0. Geometries were optimized to a minimum, and time-dependent DFT calculations[53] were performed on the optimized geometries to determine the first 80 singlet transitions for $1'$ and the first 100 singlet transitions for $1Br_2'$ and $1Cl_2'$.

Synthesis. *5-Iodoisatin.* A 250 mL three-neck flask was charged with isatin (5.0 g, 34.0 mmol) and periodic acid (1.94 g, 8.50 mmol) and equipped with a condenser and addition funnel. A solution of water (14 mL), concentrated sulfuric acid (8 mL), and glacial acetic acid (150 mL) was prepared. 75 mL of this solution was added to reaction flask. Iodine (4.40 g, 17.3 mmol) was dissolved in the remaining solvent, forming a dark-brown solution, with some solid iodine which remained undissolved. The solution was transferred to the addition funnel, and the remaining solid iodine was added directly to the reaction flask. The dark-red reaction mixture was heated to 65 °C with vigorous stirring, and the iodine solution was added dropwise. After stirring of the solution overnight (~22 h), a red precipitate was observed. The reaction mixture was cooled to room temperature, filtered, and washed with 0.5 M NaHCO$_3$ and water. The crude product was purified by column chromatography (silica gel, 1:2 ethyl acetate/hexanes) to yield 5.05 g of 5-iodoisatin (18.5 mmol, 54%) as a red solid. ^{1}H NMR (300 MHz, DMSO-d_6) δ 6.75 (d, J_1 = 8.1 Hz, 1H), 7.76 (s 1H), 7.88 (d, J_1 = 8.1 Hz, 1H), 11.10 (s, 1H, N−H). ^{13}C NMR (100 MHz, DMSO-d_6) δ 85.36, 114.57, 119.93, 132.37, 145.74, 149.93, 158.66, 183.04.

5-Iodoisoindigo. Glacial acetic acid (68 mL) and concentrated hydrochloric acid (0.34 mL) were added to a 250 mL round-bottom flask containing 5-iodoisatin (5.05 g, 18.5 mmol) and oxindole (2.55 g, 19.2 mmol). The mixture was heated to reflux and stirred for 24 h. The resultant black mixture was cooled to 0 °C and filtered. The solids were washed with water, ethanol, and ethyl acetate, and dried under vacuum to yield 6.90 g (17.8 mmol, 96%) of 5-iodoisoindigo as a dark-purple solid which was used without further purification. ^{1}H NMR (400 MHz, DMSO-d_6) δ 6.70 (d, J_1 = 8.4 Hz, 1H), 6.86 (d, J_1 = 8.0 Hz, 1H), 6.97 (dd, J_1 = 8.0 Hz, J_1 = 8.0 Hz, 1H), 7.36 (dd, J_1 = 7.6 Hz, J_1 = 7.6 Hz, 1H), 7.67 (d, J_1 = 8.0 Hz, 1H), 9.05 (d, J_1 = 8.4 Hz, 1H), 9.46 (s, 1H), 10.92 (s, 1H, N−H), 11.01 (s, 1H, N−H). ^{13}C NMR (100 MHz, DMSO-d_6) δ 84.9, 110.6, 112.8, 122.2, 122.4, 124.8, 130.5, 132.7, 134.1, 135.5, 138.0, 141.2, 144.4, 145.4, 169.3, 169.9.

N,N′-Dihexyl-5-iodoisoindigo. 5-Iodoisoindigo (6.60 g, 17.0 mmol) and 95% sodium hydride (897 mg, 37.4 mmol) were added to a flame-dried 1 L Schlenk flask under nitrogen. Dry DMF (645 mL) was added, and the solution was stirred at room temperature under an open nitrogen atmosphere (an open needle was placed in the septum and a nitrogen stream was maintained). After 1 h the solution had turned dark

brownish-yellow. 1-Iodohexane (5.02 mL, 34.0 mmol) was added, and the flask was sealed and stirred for 18 h. Brine was added and the mixture was extracted three times with ethyl acetate. The combined organic layers were washed three times with brine and dried over MgSO$_4$. The crude product was purified by column chromatography (silica gel, 1:25 ethyl acetate/hexanes) to yield 5.37 g (9.65 mmol, 56.8%) of *N,N′-dihexyl-5-iodoisoindigo* as a red solid. ^{1}H NMR (400 MHz, CDCl$_3$) δ 0.86−0.91 (m, 6H), 1.26−1.40 (m, 12H), 1.63−1.74 (m, 4H), 3.73−3.79 (m, 4H), 6.58 (d, J_1 = 8.4 Hz, 1H), 6.79 (d, J_1 = 8.0 Hz, 1H), 7.04 (dd, J_1 = 8.0 Hz, J_1 = 8.0 Hz, 1H), 7.36 (dd, J_1 = 7.6 Hz, J_1 = 7.6 Hz, 1H), 7.66 (d, J_1 = 8.0 Hz, 1H), 9.16 (d, J_1 = 8.4 Hz, 1H), 9.57 (s, 1H). ^{13}C NMR (100 MHz, CDCl$_3$) δ 26.65, 13.99, 22.50, 27.33, 31.47, 40.06, 84.63, 108.00, 109.73, 121.43, 122.18, 123.62, 130.17, 131.71, 132.87, 134.87, 137.99, 140.41, 143.99, 145.09, 167.16, 167.60. TOF-MS (DART +) m/z 557.2 [M + H]$^+$.

2,5-Bis[5-(N,N′-dihexylisoindigo)]tellurophene (1). A 25 mL flame-dried Schlenk flask was charged with N,N′-dihexyl-5-iodoisoindigo (200 mg, 0.359 mmol), Pd(PPh$_3$)$_4$ (19.3 mg, 0.0167 mmol), and copper iodide (6.4 mg, 0.0334 mmol), and placed under vacuum. Dry DMF (8 mL) was degassed by bubbling nitrogen through for 45 min. A nitrogen atmosphere was introduced to the Schlenk flask, and the DMF was added. The mixture was stirred for several minutes. 2,5-Bis-(trimethylstannyl)tellurophene (84.4 mg, 0.167 mmol) was then added, and the deep-red reaction mixture was heated to 60 °C for 16 h until the color changed to dark brown. The flask was removed from the heat and allowed to cool to room temperature. Methanol was added, and the brown precipitate was collected by vacuum filtration. The crude product was redissolved in a minimum amount of dichloromethane, recrystallized by addition to cold methanol, and centrifuged to remove any unreacted starting material, yielding 71 mg of the desired product (0.068 mmol, 41%). ^{1}H NMR (500 MHz, CDCl$_3$) δ 0.84−0.94 (m, 12H), 1.25−1.47 (m, 24H), 1.68−1.75, (m, 8H), 3.80 (q, J_1 = 7.5 Hz, 8H), 6.76 (d, 8.0 Hz, 2H), 6.80 (d, J_1 = 8.0 Hz, 2H), 7.05 (dd, J_1 = 8.0 Hz, J_1 = 8.0 Hz, 2H), 7.36 (dd, J_1 = 7.5 Hz, J_1 = 7.5 Hz, 2H), 7.47 (d, J_1 = 8.5 Hz, 2H), 7.86 (s, J_{Te} = 20.0 Hz, 2H), 9.19 (d, J_1 = 8.0 Hz, 2H), 9.53 (s, 2H). ^{13}C NMR (125 MHz, CDCl$_3$) δ 14.19, 14.24, 22.70, 22.75, 26.85, 26.88, 27.59, 27.68, 31.69, 31.71, 40.19, 40.42, 108.07, 108.19, 121.81, 122.24, 122.36, 128.07, 130.19, 130.73, 132.69, 133.19, 133.53, 134.51, 134.81, 144.03, 145.15, 147.36, 167.87, 168.01. MALDI-TOF MS (LD$^+$) m/z 1038.6. CHN: C$_{60}$H$_{68}$N$_4$O$_4$Te·H$_2$O Expected: C, 68.32; H, 6.69; N, 5.31. Found: C, 68.06; H, 6.56; N, 5.21.

Oxidative Addition. *2,5-Bis[5-(N,N′-dihexylisoindigo)]-dibromotellurophene (1Br$_2$).* Compound **1** (23 mg, 0.022 mmol) was dissolved in a minimum amount of CHCl$_3$. A solution of bromine (10 μL in 1 mL CCl$_4$, 0.194 M) was prepared, and 1 equiv (0.022 mmol) was added to the solution of **1**. After the solution was stirred for 5 min, the product was recrystallized by addition to cold hexanes, centrifuged, and collected as solid **1Br$_2$**. ^{1}H NMR (500 MHz, CDCl$_3$) δ 0.84−0.94 (m, 12H), 1.25−1.47 (m, 24H), 1.69−1.76, (m, 8H), 3.80 (q, J_1 = 7.5 Hz, 8H), 6.81 (d, 8.0 Hz, 2H), 6.89 (d, J_1 = 8.5 Hz, 2H), 7.06 (dd, J_1 = 7.5 Hz, J_1 = 7.5 Hz, 2H), 7.39 (dd, J_1 = 8.0 Hz, J_1 = 8.0 Hz, 2H), 7.53 (s, J_{Te} = 5.5 Hz, 2H), 7.59 (d, J_1 = 8.5 Hz, 2H), 9.21 (d, J_1 = 8.0 Hz, 2H), 9.78 (s, 2H). ^{13}C NMR (125 MHz, CDCl$_3$) δ 14.20, 14.26, 22.70, 22.76, 26.86, 26.88, 27.58, 27.69, 31.66, 31.71, 40.29, 40.57, 108.19, 108.80, 121.64, 122.40, 123.04, 127.31, 128.63, 130.50, 131.59, 131.79, 133.23,

135.76, 137.28, 145.43, 146.03, 162.02, 167.82, 167.93. CHN: $C_{60}H_{68}N_4O_4TeBr_2 \cdot H_2O$ Expected: C, 59.33; H, 5.81; N, 4.61. Found: C, 59.17; H, 5.76; N, 4.68.

2,5-Bis[5-(N,N'-dihexylisoindigo)]dichlorotellurophene, (1Cl₂). Compound **1** (25 mg, 0.024 mmol) was dissolved in a minimum amount of $CHCl_3$. One equivalent of iodobenzene dichloride (6.63 mg, 0.024 mmol) was added to the solution of **1** and allowed to stir for 1 h. The product was recrystallized by addition to cold hexanes, centrifuged, and collected as solid **1Cl₂**. ^1H NMR (500 MHz, $CDCl_3$) δ 0.84−0.94 (m, 12H), 1.25−1.47 (m, 24H), 1.68−1.76, (m, 8H), 3.80 (q, J_1 = 7.5 Hz, 8H), 6.80 (d, 8.0 Hz, 2H), 6.88 (d, J_1 = 8.0 Hz, 2H), 7.05 (dd, J_1 = 7.5 Hz, J_1 = 7.5 Hz, 2H), 7.38 (dd, J_1 = 7.5 Hz, J_1 = 7.5 Hz, 2H), 7.58−7.63 (m, 4H), 9.21 (d, J_1 = 8.0 Hz, 2H), 9.78 (s, 2H). ^{13}C NMR (125 MHz, $CDCl_3$) δ 14.18, 14.23, 22.67, 22.73, 26.83, 26.85, 27.54, 27.65, 31.64, 31.69, 40.26, 40.54, 108.18, 108.79, 121.59, 122.37, 123.03, 127.15, 128.72, 130.48, 131.53, 131.74, 133.21, 135.70, 136.93, 145.40, 145.97, 163.87, 167.79, 167.89. CHN: $C_{60}H_{68}N_4O_4TeCl_2 \cdot 4H_2O$ Expected: C, 61.08; H, 6.49; N, 4.75. Found: C, 61.32; H, 6.03; N, 4.78.

2,5-Bis(phenyl)dichlorotellurophene (2Cl₂). 2,5-Bis-(phenyl)tellurophene, **2**, (50 mg, 0.151 mmol) was dissolved in a minimum amount of $CHCl_3$. Two equivalents of iodine monochloride (15.8 μL, 0.302 mmol) was dissolved in a minimum amount of CCl_4. The solution containing **2** was layered over the ICl solution and allowed to slowly diffuse over several days. Orange crystals were obtained and examined by single crystal X-ray crystallography. ^1H NMR (500 MHz, $CDCl_3$) δ 7.46−7.52 (m, 8H), 7.61−7.64 (m, 4H). ^{13}C NMR (125 MHz, $CDCl_3$) δ 126.90, 127.61, 129.11, 129.85, 130.79, 132.81, 134.07, 138.35.

Titration Experiments. A 1×10^{-5} M solution of **1** was prepared (in CCl_4 for bromine titration, $CHCl_3$ for $PhICl_2$ and ICl titrations). 7.75×10^{-5} M halogen stock solutions were prepared (Br_2 and ICl in CCl_4, $PhICl_2$ in $CHCl_3$) and added in 10 μL aliquots (0.25 equiv) with stirring. The absorption spectrum was recorded after each aliquot.

Competition Experiments. 1×10^{-5} M solutions of **1Br₂** and **1Cl₂** were prepared in $CHCl_3$. Opposing halogens (ICl or Br_2, respectively) were added in increments from 7.75×10^{-5} M stock solutions in CCl_4 and monitored using optical absorption spectroscopy.

Electrochemistry. Cyclic voltammetry experiments were carried out on dilute solutions of **1** and **1Br₂** in DCM in the glovebox, using 0.1 M tetrabutylammonium hexafluorophosphate as the electrolyte. The setup involved a platinum wire counter electrode, platinum gauze working electrode, and silver wire pseudoreference electrode. Scans were carried out from −1.25 to 1.25 V at a scan rate of 100 mV/s. Cyclic voltammograms were obtained for **1** and **1Br₂** both with and without ferrocene added as an internal reference. The oxidation and reduction potentials were obtained by taking the $E_{1/2}$ of oxidation and reduction peaks, and subtracting $E_{1/2}$ of the ferrocene peaks to give a potential versus the ferrocene/ferrocenium redox couple. To convert to potentials referenced to the normal hydrogen electrode (NHE), 0.4 V was added to the potential versus ferrocene.[76] To convert to potentials referenced to vacuum, 4.5 V was added to the potential versus NHE (see Table S3, Supporting Information for conversions).[77]

Thermal Reductive Elimination. Thin films of **1Br₂** and **1Cl₂** were spin-cast at 1000 rpm onto glass slides from solution (∼2 mg/mL in $CHCl_3$). The films were heated on a hot plate set to 140 °C, and the solid-state optical absorption spectrum was recorded at several time intervals. For NMR spectroscopy experiments, 5 mL round-bottom flasks containing ∼2.5 mg of **1Br₂** or **1Cl₂** were heated in a 140 °C hot oil bath. Experiments were carried out in air as well as under nitrogen flow with an open needle. After cooling, the samples were dissolved in $CDCl_3$ and a ^1H NMR spectrum was obtained. TE experiments monitored by TGA were performed on **1** (control), **1Br₂**, and **1Cl₂**. The samples were heated under nitrogen to 200 °C at a rate of 5 °C/min and held at 200 °C for 2 h.

Photoreductive Elimination. Photolysis experiments were carried out using 505 nm Rebel LEDs mounted on a Tri-Star CoolBase with 7.2 W output from Luxeon Star LEDs. The LED assembly was mounted onto a high efficiency heatsink and operated at constant current using a 700 mA driver. Experiments were carried out with a cooling fan. Solutions of **1Br₂** and **1Cl₂** (∼1×10^{-5} M) in dry, degassed $CHCl_3$ with 0.1 M halogen trap (1-hexene or DMBD) were irradiated and monitored periodically using optical absorption spectroscopy. Similar experiments were also carried out under ambient conditions without drying the solvent. For NMR spectroscopy experiments, ∼2 mg/mL solutions in dry, degassed $CHCl_3$ were prepared with 2 M halogen trap in a dry 10 mL Schlenk flask under nitrogen. Samples were irradiated (15 h for 1-hexene, 5 h for DMBD), after which the solvent and excess trap were removed by evaporation. The solid products were dissolved in $CDCl_3$ and analyzed by ^1H NMR spectroscopy. Photolysis at 0 °C was carried out in an NMR tube submerged in a beaker containing isopropanol and irradiated through the beaker wall. The bath was maintained at 0 °C using a Thermo Scientific EK45 immersion cooler.

Quantum Yield Determination. Quantum yield experiments were carried out using potassium ferrioxalate standard actinometry.[73−75] Standard and unknown samples were irradiated using the same 505 nm LED used for the photolysis reactions. Full experimental details for quantum yield measurements can be found in the Supporting Information.

■ ASSOCIATED CONTENT

Ⓢ Supporting Information

Additional experimental, computational, and crystallographic data are available free of charge via the Internet at http://pubs.acs.org.

■ AUTHOR INFORMATION

Corresponding Author

*E-mail: dseferos@chem.utoronto.ca.

Notes

The authors declare no competing financial interest.

■ ACKNOWLEDGMENTS

■ REFERENCES

(1) Heyduk, A. F.; Nocera, D. G. *Science* **2001**, *293*, 1639−1641.

(2) Teets, T. S.; Nocera, D. G. *Chem. Commun.* **2011**, *47*, 9268−9274.

(3) Esswein, A. J.; Nocera, D. G. *Chem. Rev.* **2007**, *107*, 4022−4047.

(4) Esswein, A. J.; Veige, A. S.; Nocera, D. G. *J. Am. Chem. Soc.* **2005**, *127*, 16641−16651.

(5) Valdez, C. N.; Dempsey, J. L.; Brunschwig, B. S.; Winkler, J. R.; Gray, H. B. *Proc. Natl. Acad. Sci. U.S.A.* **2012**, *109*, 15589−15593.

(6) Dempsey, J. L; Brunschwig, B. S.; Winkler, J. R.; Gray, H. B. *Acc. Chem. Res.* **2009**, *42*, 1995−2004.

(7) Dempsey, J. L; Esswein, A. J.; Manke, D. R.; Rosenthal, J.; Soper, J. D.; Nocera, D. G. *Inorg. Chem.* **2005**, *44*, 6879−6892.

(8) Spokoyny, A. M.; Reuter, M.; Stern, C. L; Ratner, M. A.; Seideman, T.; Mirkin, C. A. *J. Am. Chem. Soc.* **2009**, *131*, 9482−9483.

(9) Zhao, H.; Gabbaï, F. P. *Nat. Chem.* **2010**, *2*, 984−990.

(10) Lin, T-P; Gabbaï, F. P. *Angew. Chem., Int. Ed.* **2013**, *52*, 3864−3868.

(11) McCormick, T. M.; Jahnke, A. A.; Lough, A. J.; Seferos, D. S. *J. Am. Chem. Soc.* **2012**, *134*, 3542−3548.

(12) Jahnke, A. A.; Howe, G. W.; Seferos, D. S. *Angew. Chem., Int. Ed.* **2010**, *49*, 10140−10144.

(13) Hollinger, J.; DiCarmine, P. M.; Karl, D.; Seferos, D. S. *Macromolecules* **2012**, *45*, 3772−3778.

(14) Hollinger, J.; Sun, J.; Gao, D.; Karl, D.; Seferos, D. S. *Macromol. Rapid Commun.* **2013**, *34*, 437−441.

(15) Martin, C. D.; Le, C. M.; Ragogna, P. J. *J. Am. Chem. Soc.* **2009**, *131*, 15126−15127.

(16) Dutton, J. L; Ontario, T.; Ragogna, P. J. *Chem.—Eur. J.* **2010**, *16*, 12454−12461.

(17) Dutton, J. L.; Martin, C. D.; Sgro, M. J.; Jones, N. D.; Ragogna, P. J. *Inorg. Chem.* **2009**, *48*, 3239−3247.

(18) Dutton, J. L.; Ragogna, P. J. *Inorg. Chem.* **2009**, *48*, 1722−1730.

(19) Martin, C. D.; Ragogna, P. J. *Inorg. Chem.* **2012**, *51*, 2947−2953.

(20) Gibson, G. L.; McCormick, T. M.; Seferos, D. S. *J. Am. Chem. Soc.* **2012**, *134*, 539−547.

(21) Magdzinski, E.; Gobbo, P.; Martin, C. D.; Workentin, M. S.; Ragogna, P. J. *Inorg. Chem.* **2012**, *51*, 8425−8432.

(22) Itthibenchapong, V.; Kokenyesi, R. S.; Ritenour, A. J.; Zakharov, L. N.; Boettcher, S. W.; Wager, J. F.; Keszler, D. A. *J. Mater. Chem. C* **2012**, *1*, 657−662.

(23) Detty, M. R.; Luss, H. R. *Organometallics* **1986**, *5*, 2250−2256.

(24) Detty, M. R.; Friedman, A. E. *Organometallics* **1994**, *13*, 533−540.

(25) Detty, M. R. *Organometallics* **1991**, *10*, 702−712.

(26) Detty, M. R.; Frade, T. M. *Organometallics* **1993**, *12*, 2496−2504.

(27) Leonard, K. A.; Zhou, F.; Detty, M. R. *Organometallics* **1996**, *15*, 4285−4292.

(28) Detty, M. R.; Gibson, S. L. *Organometallics* **1992**, *11*, 2147−2156.

(29) Detty, M. R.; Gibson, S. L. *J. Am. Chem. Soc.* **1990**, *112*, 4086−4088.

(30) You, Y.; Ahsan, K.; Detty, M. R. *J. Am. Chem. Soc.* **2003**, *125*, 4918−4927.

(31) Ahsan, K.; Drake, M. D.; Higgs, D. E.; Wojciechowski, A. L.; Tse, B. N.; Bateman, M. A.; You, Y.; Detty, M. R. *Organometallics* **2003**, *22*, 2883−2890.

(32) Abe, M.; You, Y.; Detty, M. R. *Organometallics* **2002**, *21*, 4546−4551.

(33) Detty, M. R.; Higgs, D. E.; Nelen, M. I. *Org. Lett.* **2001**, *3*, 349−352.

(34) Detty, M. R.; Zhou, F.; Friedman, A. E. *J. Am. Chem. Soc.* **1996**, *118*, 313−318.

(35) He, G.; Kang, L.; Delgado, W. T.; Shynkaruk, O.; Ferguson, M. J.; McDonald, R.; Rivard, E. *J. Am. Chem. Soc.* **2013**, *135*, 5360−5363.

(36) Pittelkow, M.; Reenberg, T. K.; Nielsen, K. T.; Magnussen, M. J.; Sølling, T. I.; Krebs, F. C.; Christensen, J. B. *Angew. Chem., Int. Ed.* **2006**, *45*, 5666−5670.

(37) Patra, A.; Wijsboom, Y. H.; Leitus, G.; Bendikov, M. *Org. Lett.* **2009**, *11*, 1487−1490.

(38) Inoue, S.; Jigami, T.; Nozoe, H.; Otsubo, T.; Ogura, F. *Tetrahedron Lett.* **1994**, *35*, 8009−8012.

(39) Otsubo, T.; Inoue, S.; Nozoe, H.; Jigami, T.; Ogura, F. *Synth. Met.* **1995**, *69*, 537−538.

(40) Sugimoto, R.-I.; Yoshino, K.; Inoue, S.; Tsukagoshi, K. *Jpn. J. Appl. Phys. 1* **1985**, *24*, L425−L427.

(41) Inoue, S.; Jigami, T.; Nozoe, H.; Aso, Y.; Ogura, F.; Otsubo, T. *Heterocycles* **2000**, *52*, 159−170.

(42) Jahnke, A. A.; Djukic, B.; McCormick, T. M.; Domingo, E. B.; Hellmann, C.; Lee, Y.; Seferos, D. S. *J. Am. Chem. Soc.* **2013**, *135*, 951−954.

(43) Narita, Y.; Takeda, K. *Jpn. J. Appl. Phys. 1* **2006**, *45*, 2628−2642.

(44) Narita, Y.; Hagiri, I.; Takahashi, N.; Takeda, K. *Jpn. J. Appl. Phys.* **2004**, *43*, 4248−4258.

(45) Jahnke, A. A.; Seferos, D. S. *Macromol. Rapid Commun.* **2011**, *32*, 943−951.

(46) Cook, T. R.; McCarthy, B. D.; Lutterman, D. A.; Nocera, D. G. *Inorg. Chem.* **2012**, *51*, 5152−5163.

(47) Powers, D. C.; Chambers, M. B.; Teets, T. S.; Elgrishi, N.; Anderson, B. L.; Nocera, D. G. *Chem. Sci.* **2013**, *4*, 2880−2885.

(48) Karikachery, A. R.; Lee, H. B.; Masjedi, M.; Ross, A.; Moody, M. A.; Cai, X.; Chui, M.; Hoff, C. D.; Sharp, P. R. *Inorg. Chem.* **2013**, *52*, 4113−4119.

(49) Teets, T. S.; Nocera, D. G. *J. Am. Chem. Soc.* **2009**, *131*, 7411−7420.

(50) Teets, T. S.; Lutterman, D. A.; Nocera, D. G. *Inorg. Chem.* **2010**, *49*, 3035−3043.

(51) Cook, T. R.; Esswein, A. J.; Nocera, D. G. *J. Am. Chem. Soc.* **2007**, *129*, 10094−10095.

(52) Lin, T.-P.; Gabbaï, F. P. *J. Am. Chem. Soc.* **2012**, *134*, 12230−12238.

(53) Bauernschmitt, R.; Ahlrichs, R. *Chem. Phys. Lett.* **1996**, *256*, 454−464.

(54) Frisch, M. J. et al. *Gaussian 09*, revision A.1; Gaussian, Inc.: Wallingford, CT, 2009.

(55) McCormick, T. M.; Bridges, C. R.; Carrera, E. I.; DiCarmine, P. M.; Gibson, G. L.; Hollinger, J.; Kozycz, L. M.; Seferos, D. S. *Macromolecules* **2013**, *46*, 3879−3886.

(56) Becke, A. D. *J. Chem. Phys.* **1993**, *98*, 5648−5652.

(57) Becke, A. D. *J. Chem. Phys.* **1996**, *104*, 1040−1046.

(58) Hay, P. J.; Wadt, W. R. *J. Chem. Phys.* **1985**, *82*, 270−283.

(59) Hehre, W. J.; Ditchfield, R.; Pople, J. A. *J. Chem. Phys.* **1972**, *56*, 2257−2261.

(60) Zhu, Y.; Kulkarni, A. P.; Wu, P-T; Jenekhe, S. A. *Chem. Mater.* **2008**, *20*, 4200−4211.

(61) Jenekhe, S. A.; Lu, L.; Alam, M. M. *Macromolecules* **2001**, *34*, 7315−7324.

(62) Ward, S. E.; Harries, M.; Aldegheri, L.; Andreotti, D.; Ballantine, S.; Bax, B. D.; Harris, A. J.; Harker, A. J.; Lund, J.; Melarange, R.; Mingardi, A.; Mookherjee, C.; Mosley, J.; Neve, M.; Oliosi, B.; Profeta, R.; Smith, K. J.; Smith, P. W.; Spada, S.; Thewlis, K. M.; Yusaf, S. P. *J. Med. Chem.* **2010**, *53*, 5801−12.

(63) Mei, J.; Graham, K. R.; Stalder, R.; Reynolds, J. R. *Org. Lett.* **2010**, *12*, 660−663.

(64) Diaz, P.; Xu, J.; Astruc-Diaz, F.; Pan, H.; Brown, D. L.; Naguib, M. *J. Med. Chem.* **2008**, *51*, 4932−4947.

(65) Sweat, D. P.; Stephens, C. E. *J. Organomet. Chem.* **2008**, *693*, 2463−2464.

(66) Stephens, C. E.; Sweat, D. P. *Synthesis* **2009**, *19*, 3214−3218.

(67) Kulkarni, A. P.; Zhu, Y.; Babel, A.; Wu, P.-T.; Jenekhe, S. A. *Chem. Mater.* **2008**, *20*, 4212−4223.

(68) Kasha, M. *J. Chem. Phys.* **1952**, *20*, 71−74.

(69) McGlynn, S. P.; Sunseri, R.; Christodouleas, N. *J. Chem. Phys.* **1962**, *37*, 1818−1824.

(70) Zhang, C.; Zhao, X.-F. *Synthesis* **2007**, *4*, 551−557.

(71) Pease, R. N.; Walz, G. F. *J. Am. Chem. Soc.* **1931**, *53*, 3728−3737.

(72) Wayne, R. P.; Poulet, G.; Biggs, P.; Burrows, J. P.; Cox, R. A.; Crutzen, P. J.; Hayman, G. D.; E, J. M.; Le Bras, G.; Moortgat, G. K.; Platt, U.; Schindler, R. N. *Atmos. Environ.* **1995**, *29*, 2677−2881.

(73) Parker, C. A. *Proc. R. Soc. London, Ser. A* **1953**, *220*, 104−116.

(74) Hatchard, C. G.; Parker, C. A. *Proc. R. Soc. London, Ser. A* **1956**, *235*, 518−536.

(75) Kuhn, H. J.; Braslavsky, S. E.; Schmidt, R. *Pure Appl. Chem.* **2004**, *76*, 2105−2146.

(76) Gagné, R. R.; Koval, C. A.; Lisensky, G. C. *Inorg. Chem.* **1980**, *19*, 2855−2857.

(77) Brovelli, F.; Rivas, B. L.; Bernède, J. C.; del Valle, M. A.; Díaz, F. R.; Berredjem, Y. *Polym. Bull.* **2007**, *58*, 521−527.